Polymer-Plastics Technology and Engineering, 46: 541–548, 2007

ISSN: 0360-2559 print/1525-6111 online
DOI: 10.1080/03602550701298655

Morphology, Thermal and Mechanical Properties of Poly (Styrene-Acrylonitrile) (SAN)/Clay Nanocomposites from Organic-Modified Montmorillonite

Yibing Cai, Yuan Hu, Junfeng Xiao, Lei Song, and Weicheng Fan
State Key Laboratory of Fire Science, University of Science and Technology of China, Hefei, Anhui, P.R. China

Huaxia Deng and Xinglong Gong
CAS Key Laboratory of Mechanical Behavior and Design of Materials, Department of Mechanics and Mechanical Engineering, University of Science and Technology of China, Hefei, Anhui, P.R. China

Zuyao Chen
Department of Chemistry, University of Science and Technology of China, Hefei, Anhui, P.R. China

Poly (styrene-acrylonitrile) (SAN)/clay nanocomposites have successfully been prepared by melt intercalation method. The hexadecyl triphenyl phosphonium bromide (P16) and cetyl pyridium chloride (CPC) are used to modify the montmorillonite (MMT). The structure and thermal stability property of the organic modified MMT are, respectively characterized by Fourier transfer infrared (FT-IR) spectra, X-ray diffraction (XRD) and thermogravimetric analysis (TGA). The results indicate that the cationic surfactants intercalate into the gallery of MMT and the organic-modified MMT by P16 and CPC has higher thermal stability than hexadecyl trimethyl ammonium bromide (C16) modified MMT. The influences of the different organic modified MMT on the structure and properties of the SAN/clay nanocomposites are investigated by XRD, transmission electronic microscopy (TEM), high-resolution electron microscopy (HREM), TGA and dynamic mechanical analysis (DMA), respectively. The results indicate that the SAN cannot intercalate into the interlayers of the pristine MMT and results in microcomposites. However, the dispersion of the organic-modified MMT in the SAN is rather facile and the SAN nanocomposites reveal an intermediate morphology, an intercalated structure with some exfoliation and the presence of small tactoids. The thermal stability and the char residue at 700°C of the SAN/clay nanocomposites have remarkably enhancements compared with pure SAN. DMA measurements show that the silicate clays improve the storage modulus and glass transition temperature (Tg) of the SAN matrix in the nanocomposites.

Keywords Montmorillonite (MMT); Nanocomposites; OMT-CPC; OMT-P16; Organic-modified montmorillonite (OMT); Poly (styrene-acrylonitrile) (SAN)

Address correspondence to Yuan Hu, State Key Laboratory of Fire Science, University of Science and Technology of China, Hefei, 230026, Anhui, China. E-mail: yuanhu@ustc.edu.cn

1. INTRODUCTION

Since a nylon-6/clay hybrid material reported by the Japanese industrial research group[1] and melt-mixing method without the use of organic solvents used by Giannelis et al.[2], polymer/clay nanocomposites, as a very promising alternative to conventional filled polymers, have attracted a remarkably strong attention of academic and industrial researchers. The dispersion of these ultra-thin (1 nm) ultra- high surface area clay layers (usually less than 10 wt.%) within a polymer matrix leads to nanocomposites exhibiting markedly improved physicochemical properties, better dimensional and thermal stabilities, improved gas barrier properties and reduced flammability, compared with pure polymers or conventional microcomposites. In general, polymer layered silicate composites are of three categories; microcomposites, exfoliated composites and intercalated composites. Many of the properties associated with polymer layered silicate nanocomposites are a function of the extent of exfoliation of the individual clay sheets. Among these enhanced properties, mechanical and gas barrier properties are related to the types of clay dispersion in the polymer, while fire retardant property has been ascribed to the formation of a barrier which impedes mass transport of degrading polymer species and insulates the flame from the underlying polymer[3–6].

Poly (styrene-acrylonitrile) (SAN) is a widely used engineering thermoplastic owing to its desirable properties, which include good mechanical properties, chemical resistance and easy processing characteristics. It has many important applications, such as the fittings of mobile

industry and home appliance, instrument panel, various switches and lamina of the fanner, etc. Furthermore, SAN is the matrix phase of the multiphase ABS. Therefore, the studies of SAN-layered silicate nanocomposites are very important, which can be used as a simple and useful model for understanding the more complex ABS-layered silicate nanocomposite system. The influences of the organic treatment on formation, morphology and properties of polymer nanocomposites are highly important, since the organic treatment is the interface between layered silicate and the matrix polymer. A poor interface will often result in a microcomposite, or a traditional filled system. Hence, the study of different organic treatment on the clay surface can help understand how this interface affects the properties observed in the final polymer layered-silicate nanocomposites, as well as how that organic treatment gives rise to the observed nanocomposites structure[7–10]. But the temperature of the decomposition of alkyl ammonium cations in the organic modified montmorillonite is generally low. The thermal instability of alkyl ammonium modified clays mainly comes from the Hofmann elimination reaction around 200°C, producing an olefin and an amine, and leaving a proton occupying the cationic position on the clay[11,12]. The thermal instability of the ammonium salts not only alters the interface between layered silicate and the matrix polymer, but also promotes the degradation of the polymer matrix. Therefore, the preparation of high thermal stability organic-modified MMT is necessary for the well dispersed of clay in the polymer matrix.

In this article, we used hexadecyl triphenyl phosphonium bromide (P16) and cetyl pyridium chloride (CPC) to prepare the high thermal stability organic-modified montmorillonites and then prepared the SAN/clay nanocomposites via direct melt intercalation method. The structure and properties of the nanocomposites were investigated compared with the pure SAN and SAN/OMT-C16 nanocomposites.

2. EXPERIMENTAL

2.1. Materials

Poly (styrene-acrylonitrile) (SAN, 32.5–34.5 wt.% AN) was supplied as pellets by the Guoheng Chemical Company (Zhenjiang China). The original purified sodium montmorillonite (MMT, with a cation exchange capacity (CEC) of 97 meq/100g) and hexadecyl trimethyl ammonium bromide (C16) modified montmorillonite, OMT-C16, were kindly provided by Keyan Company. Hexadecyl triphenyl phosphonium bromide (P16) and cetyl pyridium chloride (CPC) were purchased from Shanghai Chemicals.

2.2. The Preparation of OMT-P16 and OMT-CPC

The P16 and CPC modified montmorillonites were prepared by cation exchange reaction of Na^+ and P16 or CPC. MMT (10 g) and P16 (5.4 g) were added to 400 ml distilled water in 500-ml flask. The mixture was stirred vigorously for 2 h at 80°C before the P16-exchanged silicates were collected by filtration. The solids were subsequently washed with hot distilled water until no halide ion could be detected by an aqueous $AgNO_3$ solution. The product was dried in a vacuum oven overnight at 80°C and then ground to obtain the OMT-P16.

The prepared procedure of OMT-CPC was similar to that for the OMT-P16. MMT (5 g) and CPC (1.72 g) were added to 400 ml distilled water in 500-ml flask and stirred vigorously for 5 h at 80°C. Then the solids were washed, dried and ground to obtain the OMT-CPC.

2.3. The Preparation of SAN/Clay Nanocomposites

The clay and the SAN pellets were dried under vacuum oven at 80°C for overnight before use. SAN was melt-mixed with clay in a twin-roll mill (XK-160, made in Jiang-su, China) for 10 min. The temperature of the mill was maintained 180°C and the roll speed was 100 rpm. The resulting samples were compressed and molded into sheets (1 and 3 mm thickness). The samples are listed in Table 1.

2.4. Characterization

The Fourier transfer infrared (FT-IR) spectra were recorded on a Nicolet MAGNA-IR 750 spectrometer by the standard KBr disk method in the range of 350–4000 cm^{-1} with a resolution of 4 cm^{-1}.

X-ray diffraction (XRD) patterns were performed on the 1 mm thick films with a Japan Rigaku D/Max-Ra rotating anode X-ray diffractometer equipped with a Cu-Ka tube and Ni filter ($\lambda = 0.1542$ nm). Transmission electron microscopy (TEM) images were obtained on a Jeol JEM-100SX transmission electron microscope with an acceleration voltage of 100 kV. High-resolution electron microscopy (HREM) images were obtained by JEOL 2010 with an acceleration voltage of 200 kV. The TEM and HREM specimens were cut at room temperature using an ultramicrotome (Ultracut-1, UK) with a diamond knife from an epoxy block with the films of the embedded nanocomposite. Thin specimens, 50–80 nm, were collected in a

TABLE 1
Formulations of SAN-clay nanocomposites

Samples	Composition
SAN1	SAN + MMT (4 wt. %)
SAN2	SAN + OMT − C16 (4 wt. %)
SAN3	SAN + OMT − P16 (4 wt. %)
SAN4	SAN + OMT − CPC (4 wt. %)

trough filled with water and placed on 200 mesh copper grids.

Thermogravimetric analyses (TGA) were carried out using a TGA50H thermoanalyzer instrument from 25–700°C using a linear heating rate of 10°C/min under nitrogen flow. The nitrogen flow was 25 ml/min. Samples were measured in a sealed alumina pan with a mass of about 10 mg.

The dynamic mechanical measurements of materials were carried out using a Tritec 2000B Dynamic Mechanical Analyser from 30–160°C with a heating rate of 5°C/min under 0.04% of deformation at 1 Hz of frequency. The samples (dimension $15 \times 9 \times 1$ mm) were molded in 180°C for 10 min under 5 Mpa of pressure.

3. RESULTS AND DISCUSSION

3.1. Characterization and Thermal Stability of Organic Modified MMT

The FT-IR spectra of the P16, MMT, OMT-P16, CPC and OMT-CPC are shown in Figs. 1 and 2, respectively. The characteristic bands of MMT are 3620, 1032, 512 and 460 cm^{-1}, corresponding to the stretching vibration of O–H, the stretching vibration of Si–O–Si, the stretching vibration of Al–O and the Si–O bending vibration of MMT, respectively. The characteristic peaks at around 3055, 1438, 1112 cm^{-1} and 2923, 2840 cm^{-1} are, respectively the stretching and bending vibrations of PPh_3 and the stretching vibration of the hexadecane from P16. The peaks at 2915, 2850 cm^{-1} and those around 1480 cm^{-1} are, respectively the characteristic bands of the symmetric and asymmetric stretching vibrations and bending vibration of methylene groups from CPC. The spectra of the organic-modified MMT (OMT-P16 and OMT-CPC) contain the characteristic bands of MMT and cationic surfactants (P16 and CPC). The results suggest that the cationic surfactants have tethered into the interlayers of the silicate clay.

XRD patterns of MMT, OMT-C16, OMT-P16 and OMT-CPC are shown in Figs. 3 and 4. XRD results prove the intercalation of cationic surfactants into the galleries of silicate clays. The peaks correspond to the (001) plane reflections of the clays. The average basal spacing of MMT increases from 1.51 nm to 3.45 nm and 2.38 nm after organic modified by P16 and CPC, respectively. The increased spacing suggests the cationic surfactants intercalate into the galleries of MMT. The interlayer spacing of OMT-C16 is 2.37 nm, which is observed at lower angle

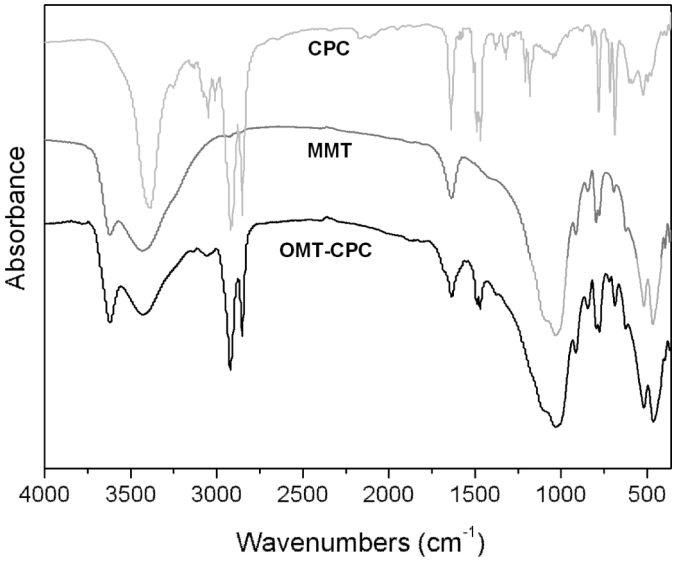

FIG. 2. FT-IR spectra of CPC, MMT and OMT-CPC.

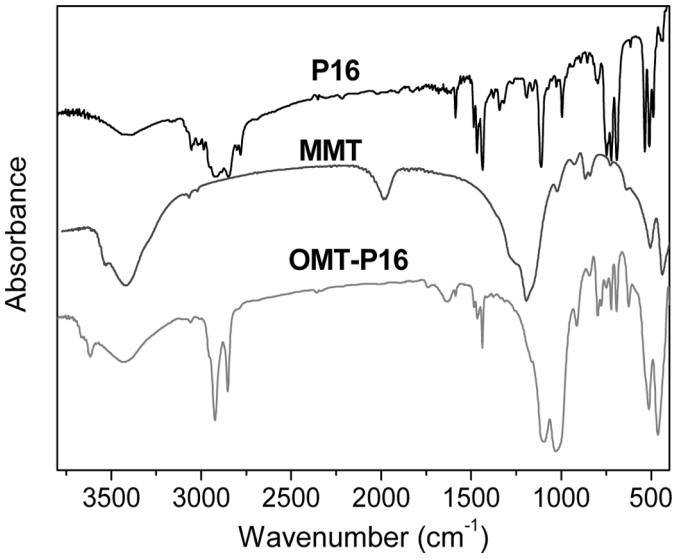

FIG. 1. FT-IR spectra of P16, MMT and OMT-P16.

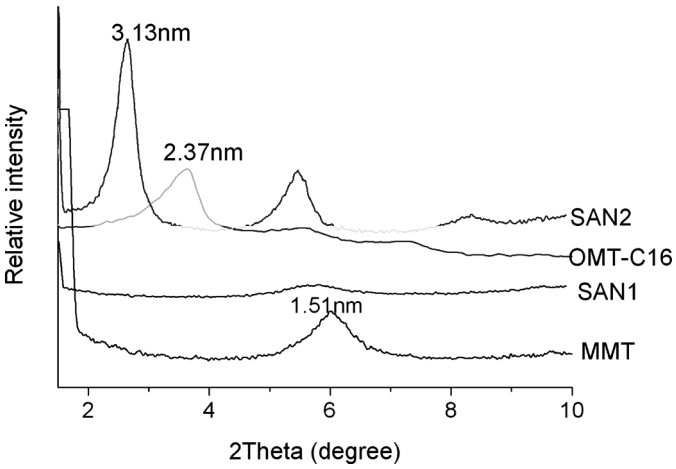

FIG. 3. XRD patterns of the MMT, OMT-C16, SAN1 and SAN2.

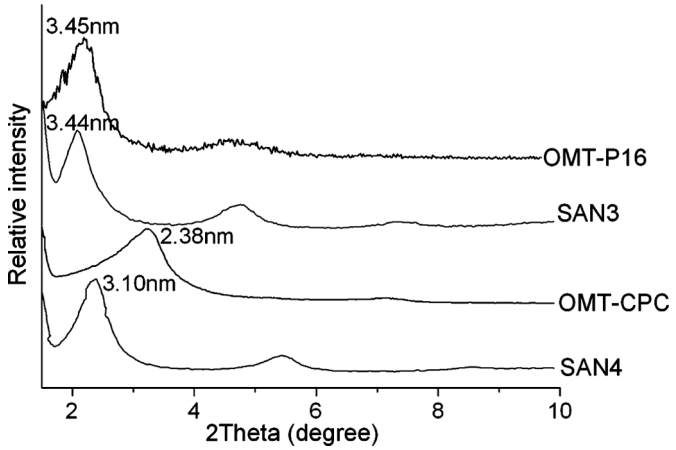

FIG. 4. XRD patterns of the OMT-P16, OMT-CPC, SAN3 and SAN4.

than that of the pristine MMT and indicates a similar cationic surfactant arrangement.

As mentioned in the introduction, the thermal instability of the ammonium salts has been a problem during the processing of thermoplastics above 200°C. The phosphonium and pyridium salt in which the Hofmann elimination is rendered difficult, may prove useful when such high temperature processing conditions are required. The high thermal stability of organic modified MMT also is important for the good clay dispersion in the polymer matrix. Because of their aromatic ring structure, phosphonium and pyridium cations have better thermal stability than ammonium cations. The thermal stability of OMT-P16 and OMT-CPC, as well as MMT and OMT-C16 is demonstrated by TGA (Fig. 5). From the TGA curves, it can be seen that the onset decomposition temperature of OMT-P16 and OMT-CPC, defined as the temperature at 2% weight loss, is respectively 243.8 and 229.4°C while the onset decomposition temperature of OMT-C16 is 193.8°C. The results

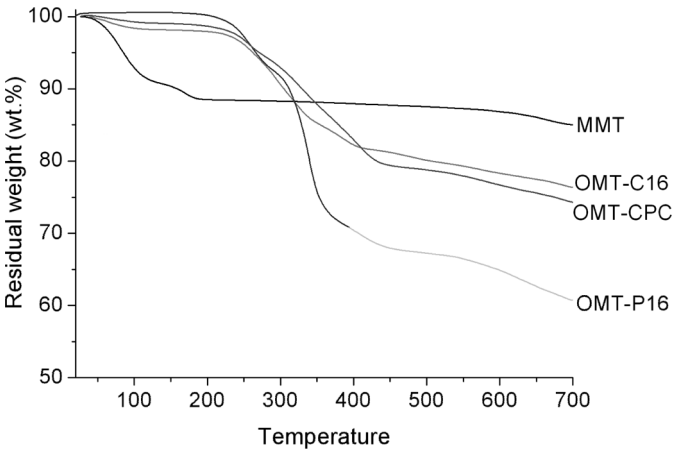

FIG. 5. TGA curves of MMT, OMT-C16, OMT-P16 and OMT-CPC.

demonstrate that the thermal stability of organic modified MMT by P16 and CPC has remarkably enhancements compared with the OMT-C16.

3.2. Structure of the SAN/Clay Nanocomposites

The XRD curves of the SAN/clay hybrids containing 4 wt.% clay is also presented in Figs. 3 and 4. The SAN1 exhibits only a weak peak corresponding to the same interlayer distance of 1.51 nm as that of pristine MMT, which indicates that SAN cannot intercalate into the gallery of MMT and results in a microcomposites without organic modification. The reasons may be that the pristine MMT is hydrophilic and the SAN matrix is hydrophobic, so that it is hard to obtain a thermodynamically homogeneous mixture of clay with SAN matrix on the molecular level. The XRD pattern of SAN2 shows that the spacing of the silicate clays increases from 2.37 nm of the OMT-C16 to 3.13 nm and remains the second diffraction peak, indicating the formation of the intercalated morphology. For SAN4, it shows that the spacing is around 3.10 nm and has an increase compared with the OMT-CPC (2.38 nm). This indicates the clay layers are intercalated in the SAN matrix. For SAN3, the interlayer spacing almost is the same as that seen in the clay itself (OMT-P16). While one might take this as indication that the polymer does not penetrate the gallery space, an alternate explanation is that the gallery space has already expanded sufficiently to permit the entry of additional material without additional expansion. The spacing is large enough to permit the entry of polymer and the similar phenomena have also reported in literatures[13,14]. Therefore XRD gives an indication of the type of hybrid that has been produced but transmission electron microscopy (TEM) is required to image the clay platelets and fully identify the type of nanocomposite that has been produced.

To further confirm the dispersion of clay in the SAN matrix, TEM investigations are required. The TEM and HREM micrographs are, respectively presented in Figs. 6 and 7. The TEM results show that the MMT dispersed phase possessed many particles in the micron size for the SAN1 (Fig. 6a) with the pristine MMT. The inability to observe individual silicate layers within the particles is consistent with the XRD result, indicating the SAN hasn't intercalated into the gallery of MMT without organic modification. For SAN2, the silicate layers are well distributed throughout the SAN matrix and some larger intercalated tactoids (multiplayer particles) are visible (Figs. 6b and 7a). This suggests that there is a greater interaction between the silicate clays and the SAN matrix than that in the SAN1. The XRD and TEM results indicate that the typically intercalated structure is formed in SAN matrix with OMT-C16. The TEM images of SAN3 and SAN4 at low magnification (Fig. 6c,d) both show uniform distribution of the organic modified clays in the SAN

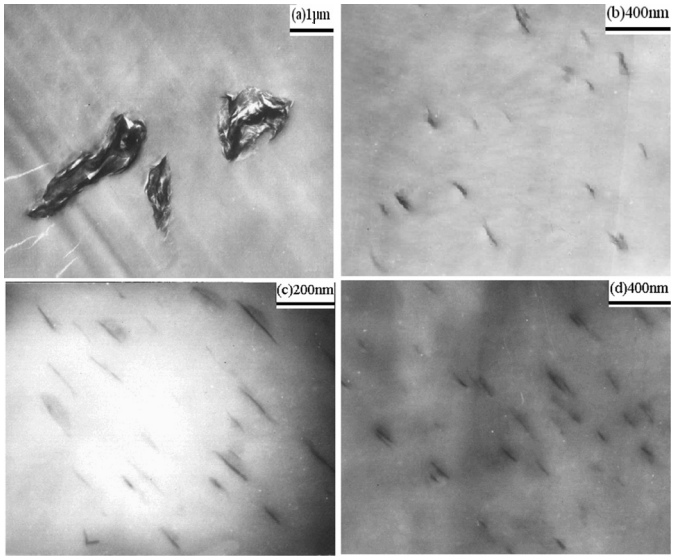

FIG. 6. TEM images of SAN/clay nanocomposites: (a) SAN1, (b) SAN2, (c) SAN3 and (d) SAN4.

matrix, but the silicate clay plate dimension is different. The clay plate sizes of the SAN3 are much slender than those of the SAN4. This may be the reason that the phenyl structure of the OMT-P16 is similar to the SAN matrix and results in better compatibility compared with the hetero-aromatic ring groups of the OMT-CPC. The difference of the morphology of the three SAN/clay nanocomposites is shown by HREM in Fig. 7. In Fig. 7a,c, the intercalated structures of SAN2 and SAN4 are confirmed by a significant number of tactoids comprised of several clay layers observed. For SAN3 (Fig. 7b), some single clay platelets combined with a few multilayer tactoids are observed. This indicates that clay layers are partially intercalated and partially exfoliated in the SAN matrix. From the XRD and TEM results, one can conclude that the SAN/clay nanocomposites (SAN3) have a mixed nanomorphology containing both exfoliated and intercalated structures. The phenyl groups of cationic surfactant in the OMT-P16, which are similar to the SAN chains in structure, contribute to the partial exfoliation.

3.3. Thermal Stability Property of the SAN/Clay Nanocomposites

Thermal stability is an important property for which the nanocomposites morphology plays an important role. The thermal stability of pure SAN and the SAN/clay nanocomposites are analyzed by TGA. The TGA curves and the corresponding derivative curves (DTGA) are shown in Figs. 8 and 9, respectively. The 5% weight loss temperature ($T_{-5\,wt.\%}$), the midpoint weight loss temperature ($T_{-50\,wt.\%}$), the maximum decomposition temperature (T_{max}) and the char residue at 700°C are listed in Table 2. Evidently, the thermal decomposition of the SAN/clay nanocomposites shifts toward a higher temperature range than that of the pure SAN, which confirms the enhancement of thermal stability of intercalated SAN/nanocomposites. A remarkable effect is found for the nanocomposites and is likely to be due to an ablative reassembling of the silicate layers which may occur on the surface of the nanocomposites creating a physical protective barrier on the surface of the material. Meanwhile, the silicate clay layers act as a superior insulator and as a mass-transport barrier to the volatile products generated during the thermal decomposition for increasing the thermal stability[3]. After about 500°C, all curves become flat and mainly the inorganic residue (i.e., Al_2O_3, MgO, SiO_2) remains. Although the thermal stability of the SAN2 has notably increased as compared with the pure SAN and other SAN/clay nanocomposites, the char residue at 700°C in SAN2 is

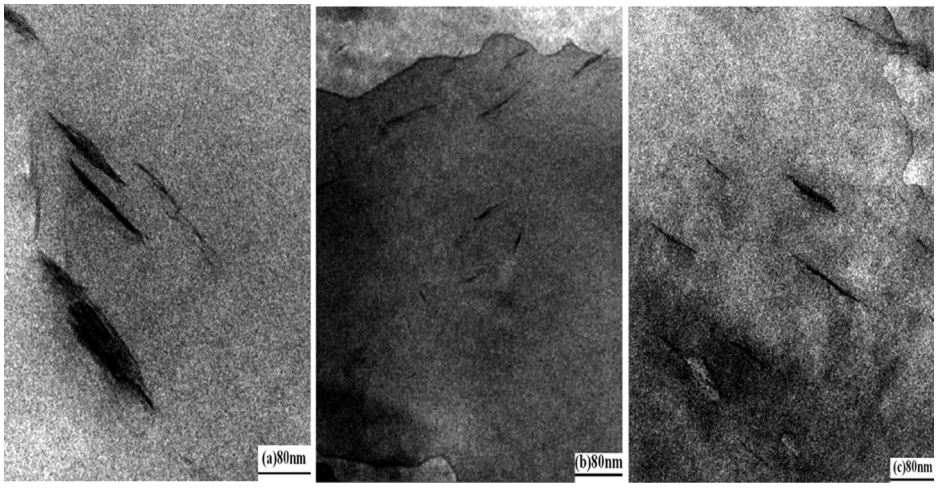

FIG. 7. HREM images of SAN/clay nanocomposites: (a) SAN2, (b) SAN3 and (c) SAN4.

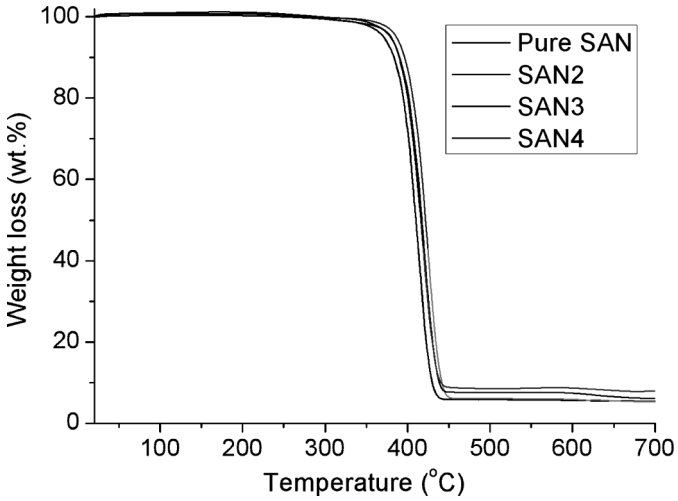

FIG. 8. TGA curves of the pure SAN, SAN2, SAN3 and SAN4.

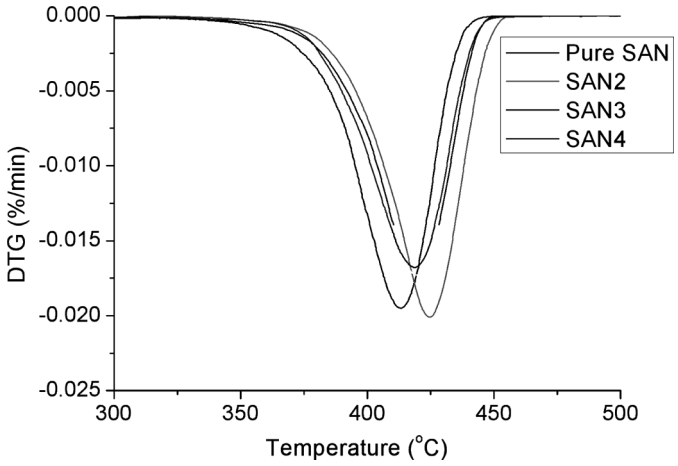

FIG. 9. DTGA curves of the pure SAN, SAN2, SAN3 and SAN4.

lower than that in pure SAN. The possible reason is that the Hofmann elimination reaction of alkyl ammonium cations accelerate the degradation of SAN at elevated temperature[15,16]. Table 2 shows that the thermal stability of the SAN2 is higher than that of the SAN3. The $T_{-5\,wt.\%}$ and T_{max} of the SAN2 increase, respectively 7 and 5°C compared with the SAN3. This is because the nanocomposites morphology plays an important role. The clay layers are intercalated in the SAN2, then intercalated with partially exfoliated in the SAN3. The intercalated clay layers are found to be better thermal stabilizers than the exfoliated ones. The similar results are presented in a study of poly (etherimide) nanocomposites[17].

TABLE 2
The TGA and DTGA data SAN and SAN-clay nanocomposites

Samples	$T_{-5\,wt.\%}$ (°C)	$T_{-50\,wt.\%}$ (°C)	T_{max} (°C)	Char (700°C)
Pure SAN	371.4	410.2	413.4	5.39
SAN2	386.5	421.7	424.8	5.22
SAN3	379.5	417.2	419.8	6.13
SAN4	380.1	416.2	418.9	7.86

3.4. Dynamic Mechanical Aanalysis of the SAN/Clay Nanocomposites

Dynamic mechanical analysis (DMA) measures the response of a given material to a cyclic deformation (usually tension or three-point flexion type deformation) as a function of the temperature. DMA results are expressed by three main parameters[6]; (i) the storage modulus (E′), corresponding to the elastic response to the deformation; (ii) the loss modulus (E″), corresponding to the plastic response to the deformation and (iii) tan δ, that is the (E′/E″) ratio, useful for determining the occurrence of molecular mobility transitions such as the glass transition temperature (Tg). The dynamic mechanical behaviors of the SAN/clay nanocomposites are studied. The curves of the storage modulus and glass transition temperature are shown in Figs. 10 and 11, respectively. The storage modulus at 30°C of the pure SAN and SAN/clay nanocomposites are, respectively 1.417×10^9 Pa and 2.796×10^9 Pa (SAN2), 3.491×10^9 Pa (SAN3), and 1.572×10^9 Pa (SAN4). The incorporation of silicate clays to SAN produces a remarkable increase in storage modulus compared to pure SAN. The well dispersed silicate clay in SAN matrix causes the enhancements and the storage modulus of the SAN3 is higher than that of the SAN2. This is relative to the different structures of SAN/clay nanocomposites. As mentioned in the structure of the SAN/clay

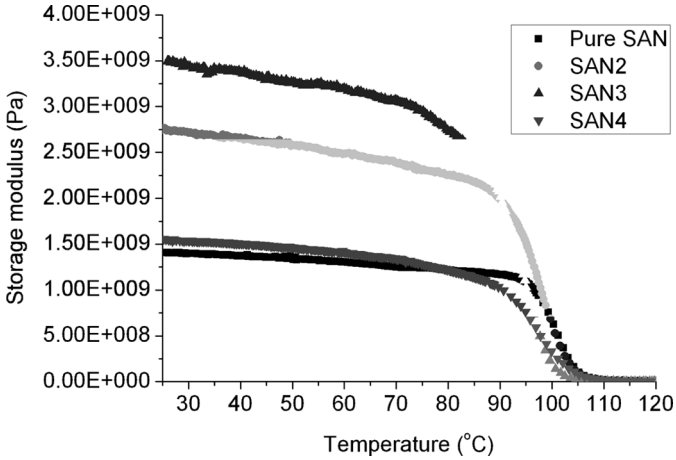

FIG. 10. Storage modulus of the pure SAN and SAN/clay nanocomposites.

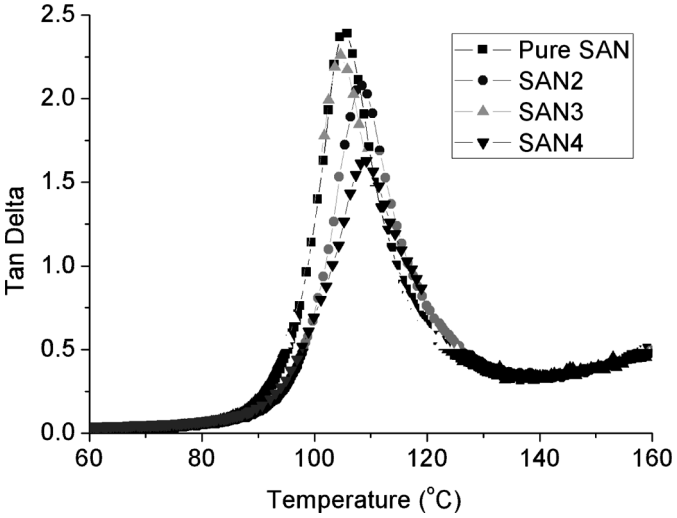

FIG. 11. Tan δ curves of the pure SAN and SAN/clay nanocomposites.

nanocomposites, the morphology of the SAN2 and SAN3 is intercalated and intercalated- exfoliated mixed structure, respectively. It is well known that the mechanical properties of the nanocomposites are enhanced relative to those of the pure polymers and that delaminated nanocomposites are enhanced relative to intercalated system[6]. The glass transition temperature (Tg) of each nanocomposites is obtained from the maximum temperature of tan δ in Fig. 11. The Tg of the pure SAN, SAN2 and SAN4 is 105.8, 108.4 and 109.2°C, respectively. The increase of Tg obtained from those SAN/clay nanocomposites is mainly due to SAN copolymers intercalated into the silicate layers of clay; the confined polymer chains in clay galleries are not completely free and the consequence of the increased thermal insulation effect of clay[18,19]. However, The Tg of the SAN3 (104.6°C) is slightly lower than the pure SAN (105.8°C). The decrease of the Tg may be considered mainly due to the excessive cationic surfactant (P16) of the OMT-P16 that exists in the SAN matrix. The plasticizing effect of the excessive P16 leads to the drop of Tg[20,21]. The Tg change of the SAN/clay nanocomposites accord with the thermal stability analysis, namely the intercalated clay layers are found to be better thermal stabilizers than the exfoliated ones.

4. CONCLUSIONS

SAN/clay nanocomposites are prepared by direct melt intercalation using hexadecyl triphenyl phosphonium bromide (P16) and cetyl pyridium chloride (CPC) modified montmorillonite (MMT), which has higher thermal stability than hexadecyl trimethyl ammonium bromide modified MMT (OMT-C16). The characterizations of the morphology and properties of the nanocomposites are carried out by XRD, TEM, HREM, TGA and DMA. The results show that the exfoliated-intercalated is formed for the SAN nanocomposites with OMT-P16 and an intercalated structure is only formed for the SAN nanocomposites with OMT-CPC and OMT-C16. The thermal stability of the SAN/clay nanocomposites has remarkably enhancements compared with the pure SAN. The DMA measurements show that the silicate clays improve the storage modulus and glass transition temperature (Tg) of the SAN matrix in the nanocomposites. It is found that the thermal stability of the intercalated nanocomposites is superior to that of the exfoliated-intercalated nanocomposites and then the opposition is embodied in the storage modulus.

ACKNOWLEDGEMENT

The work was financially supported by the National Natural Science Foundation of China (No.50476026), Specialized Research Fund for the Doctoral Program of Higher Education (20040358056) and program for New Century Excellent Talents in University.

REFERENCES

1. Usuki, A.; Kojima, Y.; Kawasumi, M.; Okada, A.; Kurauchi, T.; Kamigatio, O. Synthesis of nylon 6-clay hybrid. J. Mater. Res. **1993**, *8*, 1179–1184.
2. Vaia, R.A.; Ishii, H.; Giannelis, E.P. Synthesis and properties of 2-dimensional nanostructure by direct intercalation of polymer melts in layered silicates. Chem. Mater. **1993**, *5*, 1694–1696.
3. Gilman, J.W.; Jakson, C.L.; Morgan, A.B.; Harris, R.H.; Manias, E.; Giannelis, E.P.; Wuthenow, M.; Hilton, D.; Philips, S.H. Flammability properties of polymer-layered-silicate nanocomposites: Polypropylene and polystyrene nanocomposites. Chem. Mater. **2000**, *12*, 1866–1873.
4. Devaux, E.; Bourbigot, S.; El Achari, A. Crystallization behavior of PA-6 clay nanocomposite hybrid. J. Appl. Polym. Sci. **2002**, *86*, 2416–2423.
5. Lan, T.; Kaviratna, P.D.; Pinnavaia, T.J. On the nature of polymide clay hybrid composites. Chem. Mater. **1994**, *6*, 573–575.
6. Alexander, M.; Dubois, P. Polymer-layered silicate nanocomposites: Preparation, properties and uses of a new class of materials. Mater. Sci. Eng. **2000**, *28*, 1–63.
7. Chu, L.L.; Anderson, S.K.; Harris, J.D.; Beach, M.W.; Morgan, A.B. Styrene-acrylonitrile (SAN) layered silicate nanocomposites prepared by melt compounding. Polymer **2004**, *45*, 4051–4061.
8. Bourbigot, S.; Vanderhart, D.L.; Gilman, J.W.; Bellayer, S.; Stretz, H.; Paul, D.R. Solid state NMR characterization and flammability of styrene-acrylonitrile copolymer montmorillonite nanocomposite. Polymer **2004**, *45*, 7627–7638.
9. Stretz, H.A.; Paul, D.R.; Li, R.; Keskkula, H.; Cassidy, P.E. Intercalation and exfoliation relationships in melt-processed poly(styrene-co-acrylonitrile)/montmorillonite nanocomposites. Polymer **2005**, *46*, 2621–2637.
10. Ko, M.B. Effects of acrylonitrile content on the properties of clay-dispersed poly(styrene-co-acrylonitrile) copolymer nanocomposite. Polym. Bull. **2000**, *45*, 183–190.
11. Xie, W.; Gao, Z.M.; Pan, W.P.; Vaia, R.; Hunter, D.L.; Singh, A. Characterization of organically modified montmorillonite by thermal techniques. Polym. Mater. Sci. Eng. **2000**, *83*, 284–285.

12. Zhu, J.; Morgan, A.B.; Lamelas, F.J.; Wilkie, C.A. Fire properties of polystyrene-clay nanocomposites. Chem. Mater. **2001**, *13*, 3774–3780.
13. Zhang, J.G.; Jiang, D.D.; Wilkie, C.A. Thermal and flame properties of polyethylene and polypropylene nanocomposites based on an oligomerically-modified clay. Polym. Degrad. Stab. **2006**, *91*, 298–304.
14. Zhang, J.G.; Jiang, D.D.; Wilkie, C.A. Fire properties of styrenic polymer-clay nanocomposites based on an oligomerically-modified clay. Polym. Degrad. Stab. **2006**, *91*, 358–366.
15. Xie, W.; Gao, Z.M.; Pan, W.P.; Hunter, D.; Singh, A.; Vaia, R. Thermal degradation chemistry of alkyl quaternary ammonium montmorillonite. Chem. Mater. **2001**, *13*, 2979–2990.
16. Pinnavaia, T.J.; Beall, G.W. *Polymer-Clay Nanocomposites*, John Wiley & Sons: New York, 2000.
17. Lee, J.; Takekoshi, T.; Giannelis, E.P. Fire retardant poly(etherimide) nanocomposites. Mater. Res. Soc. Symp. Proc. **1997**, *457*, 513–518.
18. Kim, J.W.; Jang, L.W.; Choi, H.J.; Jhon, M.S. Physical and electroresponsive characteristics of the intercalated styrene-acrylonitrile copolymer/clay nanocomposite under applied electric fields. J. Appl. Polym. Sci. **2003**, *89*, 821–827.
19. Noh, M.H.; Jang, L.W.; Lee, D.C. Intercalation of styrene-acrylonitrile copolymer in layered silicate by emulsion polymerization. J. Appl. Polym. Sci. **1999**, *74*, 179–188.
20. Choi, Y.S.; Xu, M.Z.; Chung, I.J. Synthesis of exfoliated poly(styrene-co-acrylonitrile) copolymer/silicate nanocomposite by emulsion polymerization: Monomer composition effect on morphology. Polymer **2003**, *44*, 6989–6994.
21. Choi, Y.S.; Choi, M.H.; Wang, K.H.; Kim, S.O.; Kim, Y.K.; Chung, I.J. Synthesis of exfoliated PMMA/Na-MMT nanocomposites via soap-free emulsion polymerization. Macromolecules **2001**, *34*, 8978–8985.